in vivo *29*: 207-216 (2015)

No Changes in Cerebral Microcirculatory Parameters in Rat During Local Cortex Exposure to Microwaves

HIROSHI MASUDA[1,2], SHOGO HIROTA[2], AKIRA USHIYAMA[2], AKIMASA HIRATA[3], TAKUJI ARIMA[4], HIROSHI WATANABE[4,5], KANAKO WAKE[5], SOICHI WATANABE[5], MASAO TAKI[6], AKIKO NAGAI[1] and CHIYOJI OHKUBO[2,7]

[1]*Institute of Biomaterials and Bioengineering, Tokyo Medical and Dental University, Tokyo, Japan;*
[2]*Department of Environmental Health, National Institute of Public Health, Saitama, Japan;*
[3]*Department of Computer Science and Engineering, Nagoya Institute of Technology, Aichi, Japan;*
[4]*Department of Electrical and Electronics Engineering, Tokyo University of Agriculture and Technology, Tokyo, Japan;*
[5]*Electromagnetic Compatibility Laboratory, Applied Electromagnetic Research Institute, National Institute of Information and Communications Technology, Tokyo, Japan;*
[6]*Department of Electrical and Electronic Engineering, Tokyo Metropolitan University, Tokyo, Japan;*
[7]*Japan EMF Information Center, Tokyo, Japan*

Abstract. *The aim of this study was to determine whether cerebral microcirculatory parameters in rats were modified during local cortex exposure to a radiofrequency electromagnetic field (RF) under non-thermal conditions. The cortex tissue targeted was locally exposed to 1439 MHz RF using a figure-8 loop antenna at an averaged specific absorption rate of 2.0 W/kg in the target area for 50 min. Three microcirculatory parameters related to cerebral inflammation were measured by the cranial window method in real-time under RF exposure. No extravasation of intravenously injected fluorescent dye was observed during RF exposure. There was no significant difference either in pial venule blood flow velocity or diameter between exposed and sham-exposed rats. Histological evaluation for the brain immediately after RF exposure did not reveal any serum albumin leakage sites or degenerate neurons. These findings suggest that no dynamic changes occurred in cerebral microcirculation even during local cortex exposure under these conditions.*

In recent years, radiofrequency electromagnetic fields (RF) have been used for various purposes, such as magnetic resonance imaging, hyperthermia therapy, and telecommunications. In particular, their recent widespread use in smart-phone and WiFi systems has caused some concern about possible adverse effects on the brain. To provide protection against known adverse health effects, the International Commission on Non-Ionizing Radiation Protection (ICNIRP) established guidelines (1), specifying the basic restriction values in terms of specific absorption rate (SAR; W/kg) for tissue or whole body. For example, the restriction values (head and trunk, averaged over 10 g tissue) for local RF exposure (100 kHz-10 GHz), including the frequencies used in mobile telephony, are 2 W/kg for general public exposure and 10 W/kg for occupational exposure. The restriction value is based on physiological data obtained in animal studies and includes a safety factor of 10-50, which is enough to avoid eliciting known adverse health effects or a temperature elevation of 1˚C (1).

However, two research groups have reported that RF exposure induced physiological changes in brain functions at exposure intensities below the restriction value. One group, Salford *et al*., found serum albumin leakage in rat brain following exposure to 915 MHz RF, suggesting that this exposure had disrupted the blood–brain barrier (BBB) (2, 3). The other group, Huber *et al*., reported that in humans, the regional cerebral blood flow (rCBF) increased after exposure to 900 MHz pulse-modulated RF (4). Serum albumin leakage causes neurotoxicity in the brain, leading to neuronal degeneration (5, 6). Changes in rCBF are known to be related to migraine (7, 8) and neural/glial activity (9, 10). Therefore, these findings have often been quoted as a typical example of the adverse effects of RF exposure.

In contrast, many other investigators have failed to confirm reproducible, conclusive effects (11-15). For

Correspondence to: H. Masuda, Ph.D., Institute of Biomaterials and Bioengineering, Tokyo Medical and Dental University, 2-3-10 Kanda-surugadai, Chiyoda-ku, Tokyo, ZIP 101-0062, Japan. Tel: +81 0352808168, Fax: +81 0352808015, e-mail: bdxmsd@yahoo.co.jp

Key Words: Radiofrequency electromagnetic field, local exposure, blood–brain barrier, microcirculation, hemodynamics.

example, an international research team consisting of three different laboratories performed independent confirmation studies on serum albumin leakage. However, no serum album leakage was found after RF exposure, even using a similar experimental procedure to that of Salford *et al*. (16-18). For rCBF, Mizuno *et al*. and our group investigated the effects of RF exposure in humans and rats, respectively. RF exposure was not found to affect rCBF, even at local SARs higher than those used by Huber *et al*. (13, 14).

Nevertheless, there is still doubt about the adverse effects of RF exposure on the BBB and rCBF, particularly the possibility of dynamic variations, likely to appear as transient phenomena only during the RF exposure. Most previous studies evaluated the effects of RF after exposure not in real time during exposure.

Therefore, the aim of this study was to investigate whether dynamic variations in cerebral microcirculatory parameters, such as BBB permeability and hemodynamics, would be observed in rat brain during local cortex exposure to RF. To observe cerebral microcirculation in real time during exposure, we used intravital fluorescence microscopy developed for rats (19) and a figure-8 loop antenna, which provides local cortex exposure (20). Here we report that no changes were found in microcirculatory parameters even during local exposure at 2.0 W/kg local SAR.

Materials and Methods

Animals. Male Sprague-Dawley rats (n=27, 459±7 g; Tokyo Laboratory Animals Science Co., Ltd, Tokyo, Japan) were used for this experiment. They were fed a standard pellet diet and given water *ad libitum*, housed in an animal room with a 12-h light/dark cycle at a temperature of 23.0±1˚C and a relative humidity of 50±10%. All experimental procedures were conducted in accordance with the ethical recommendations for animal experiments, which was approved by the local Ethics Committee of the National Institute of Public Health, Japan.

Preparation of closed cranial window (CCW). The CCW setup was implanted into the parietal region of each rat (Figure 1A). The CCW, developed to observe pial microcirculation under RF exposure conditions (19), was made of plastic and glass, without any metal parts. In brief, the rats were anesthetized with an intramuscular injection of ketamine (100 mg/kg) and xylazine (10 mg/kg). The head of each rat was fixed in a stereotaxic apparatus. After removal of hair, skin and connective tissues from the parietal region, a 7.5-mm circular skull hole was made using a dental drill. Subsequently, the *dura mater* and arachnoid were carefully removed from the cerebral surface to expose the *pia mater*. The CCW (circular cover-glass 7.0 mm in diameter) was inserted into the hole in the skull and fixed with cyanoacrylate glue. Animal experiments started at least one week after the window implantation to allow for recovery (Figure 1B).

Definition of target area and local RF exposure. The target cortex tissue was locally exposed to 1439 MHz RF (Personal Digital Cellular signal) at several averaged SARs for the target cortex using a figure-8 loop antenna.

The target area was defined as a circular area of rat parietal cortex tissue, located just under the CCW, with its center 2 mm posterior to the *bregma* and 2 mm lateral (right) of the midline. The area included the *pia mater* (7.5 mm diameter, 0.5 mm depth, Figure 1A) in which we evaluated physiological responses during local RF exposure.

SAR was numerically and experimentally evaluated for the rat by the finite difference time domain (FDTD) method, using realistic inhomogeneous rat models (20). The rat fixed in the acrylic stereotaxic apparatus was placed in the manipulator system of the antenna. The antenna was positioned 5 mm over the CCW (Figure 1B). Under these conditions, the weights of the target area and the whole brain in the rat model were 0.018 g and 2.6 g, respectively.

RF exposure intensities were estimated and set at 2.0, 7.5, 20, 75, 200, 400 W/kg SAR in the target area (TASAR). The relative values of brain- and whole-body-averaged SARs for the TASAR of 2.0 W/kg were 0.37 and 0.022 W/kg, respectively.

RF exposure was performed for 50 min at 2.0 W/kg to record physiological parameters and for 10 min at the other SARs in turn to obtain a relationship between TASAR and temperature changes in the target area and rectum (Figure 1C). Sham-exposed rats were also prepared using the same system, but without RF exposure (0 W/kg).

Real-time measurement of physiological parameters. The temperature in two regions (target area and rectum) and three microcirculatory parameters (BBB permeability, venule diameter, and blood flow velocity in venules) were measured before, during, and just after RF exposure (Figure 1C). The rats were anesthetized with an intramuscular injection of ketamine (100 mg/kg) and xylazine (10 mg/kg) and a subcutaneous injection of pentobarbital (12.5 mg/kg). The rat was placed on a heating pad circulating warmed water (42˚C) after fixing the head under the antenna, in the same position used for the numerical model mentioned above.

Temperature measurement. Temperatures in the target area and rectum were measured using an optical fiber thermometer (m600; Lumasense Technologies, Santa Clara, CA, USA). Two optical thermometer probes (0.5 mm of diameter) were independently placed on the target area under the CCW and in the rectum. Temperatures were recorded continuously throughout the experiment, including the 50 min exposure at 2.0 W/kg TASAR in sham- and RF-treated groups (n=3 animals each).

After the 50-min exposure period, the temperatures were measured continuously during 10 min-RF exposures at different TASARs (7.5, 20, 75, 200, 400 W/kg), to obtain a relationship between TASARs and temperature variations.

Intravital fluorescence microscopy. Three microcirculatory parameters were monitored through the CCW using an intravital fluorescence microscopic system, consisting of a fluorescence binocular microscope (SZX; Olympus Optical Co. Ltd, Tokyo, Japan), an image-intensified camera (C2400-80; Hamamatsu Photonics K.K., Hamamatsu, Japan), and high-speed camera (FASTCAM-NET; Photron Ltd, Tokyo, Japan), combined with an image-intensifier (VS4-1845; International Ltd, Dulles, VA , USA). The light source was a mercury lamp (U-ULH; Olympus Optical Co. Ltd). The filter cube had a 490 nm excitation filter. The images of the pial microvascular bed were recorded on a video recorder (WV-DR7; Sony, Tokyo, Japan) equipped with a timer (VTG-33; FOR.A Co. Ltd, Tokyo, Japan). All the images were digitized and later analyzed off-line using software (Image Quest, Hamamatsu Photonics K.K.).

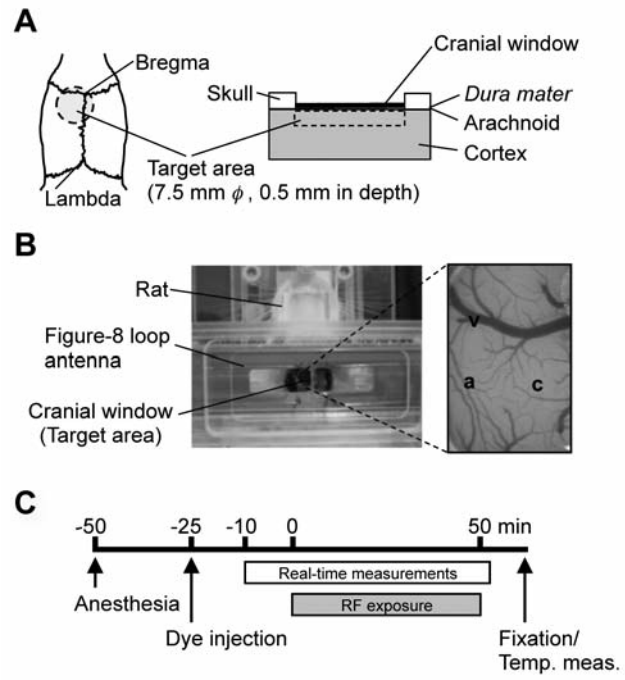

Figure 1. *Experimental design. A: Location of the target area on the rat parietal cortex. A closed cranial window was implanted on the target area through the open skull. B: Location of antenna and overview of the pial microvessels. The antenna was placed exactly over the parietal region using a manipulator. Rat pial microcirculation was observed through holes in the antenna in real-time using intravital microscopy. a: Arteriole, v: venule, c: capillary. C: Experimental procedure. The closed cranial window was implanted in the rat parietal region at least one week before the experiment.*

BBB permeability. As in a previous study (19), BBB permeability was evaluated as changes in the intensity of extravasated fluorescence dye. In brief, after intravenous injection of fluorescein isothiocyanate (FITC)-dextran (70 kDa, 25 mg/kg; Sigma-Aldrich Co., St. Louis, MO, USA), the image of the *pia mater* was recorded through an intravital fluorescence microscope with a fluorescent excitation wavelength of 490 nm. An arbitrary area of the *pia mater* was chosen as the region of interest (ROI; 0.19 mm^2, 1-3 areas per animal). The average fluorescence intensity of the ROI was measured off-line every 10 min.

To confirm whether our observation systems detected extravasated dye *in vivo*, we treated a rat with osmotic shock to the brain. Prior to intravital observation, the left internal carotid artery of the rat was catheterized. Mannitol solution (25%) was injected through the catheter (28 μl/s for 3 min) without RF exposure 25 min after dye injection. The fluorescence image of the *pia mater* was recorded and its average fluorescence intensity measured off-line every 10 min.

Hemodynamic changes. To evaluate the hemodynamics in the pial venule, its diameter and blood flow velocity were measured in postcapillary (8≤d<30 μm) and collecting venules (30≤d≤50 μm) and measurements were compared to investigate the variations in each pial venule.

Venule diameter was measured on the fluorescence images taken to assess BBB permeability. In each animal, 11-12 pial venules (8≤d≤50 μm) were selected and the ratio of final to initial diameter at −10 min from RF exposure was recorded. The change in diameter was averaged in each animal to obtain the average change within the target area for the animal, and then compared between two groups (n=9 animals per each group).

Blood flow velocity was measured using the dual-slits method developed by our team (21). In brief, the fluorescence motion images of blood flow in the pial venule were recorded using a high-speed camera (500 frames/s) every 10 min after the intravenous injection of FITC-dextran. Using the image software, two square slits were placed on the image of a pial venule, 30 μm apart. The fluorescence intensity of each slit was averaged for each image frame. The cross-correlation function, calculated using the averaged intensity changes in the two slits, produced the time intervals for erythrocytes passing between the two slits. The blood flow velocity was then calculated using the distance between the two slits and the time interval. We selected 4-12 pial venules (8≤d≤50 μm) in each animal and recorded the ratio to the initial velocity at −10 min of the RF exposure. The change in velocity was averaged in each animal to obtain the average change within the target area for the animal, and then compared between the two groups (n=8-10 animals per each group).

Histological examination of brain. Rat brain exposed to RF was histologically examined to detect traces which would be caused by dynamic changes in the microcirculatory parameters. Immediately after the last measurements of microcirculatory parameters, the rat was transcardially perfused with 4% paraformaldehyde (PFA) in phosphate-buffered saline (PBS). After the perfusion, the rat body was kept without any traumatic manipulation for at least 18 h at 4˚C. The brain was then removed from the skull and immersed in PBS containing 4% PFA. Two vertical cryosections (10 μm-thick) were taken from the frontal (between bregma −0.8 mm and −1.2 mm) and middle (between bregma −2.0 mm and −5.0 mm) lobes of the brain using a cryostat. The sections were stained as described below.

Immunohistochemistry of serum albumin was used to detect albumin leakage sites and neurons indicating albumin intake. The sections were immersed in tris buffered saline (TBS) (S3006; Dako Japan Inc., Tokyo, Japan) and endogenous peroxidase activity was inhibited by incubation in a blocking reagent (S2001; Dako) for 5 min. After the sections were washed in TBS, the background was blocked with 1% bovine serum albunin in TBS for 30 min. Then the sections were incubated with a 1:100 dilution of rabbit polyclonal antibody to human albumin (A0001; Dako) for 1 h. The sections were then washed in TBS and incubated with a 1:100 dilution of goat polyclonal antibody to rabbit IgG labeled with horseradish peroxidase (PO448; Dako) for 30 min. The presence of antibodies was detected using a diaminobenzidine (DAB) liquid system (K3466; Dako). After chromogen reaction of DAB, the sections were washed in distilled water and then stained with hematoxylin to identify nuclei.

Fluoro-Jade B staining was used to detect degenerated neurons in the brain section. After treatment with three different solutions (1% NaOH and 80% ethanol for 5 min, 70% ethanol for 2 min, and 0.06% potassium permanganate for 10 min) in turn, the section was rinsed and stained with 0.0004% Fluoro-Jade B (AG310; Chemicon International, Inc., Temecula, CA, USA) in 0.1% acetic acid solution for 20 min. After rinsing with distilled water, the section was completely dried, immersed in xylene, and the mounted using mounting medium. To confirm that the Fluoro-Jade B staining method was valid, a rat brain

injured by hyperthermia was prepared as a positive control. Heat injury was elicited by maintaining the temperature of the target area at 43-46˚C for 18 min under deep anesthesia. Brain fixation and removal were carried out as described above.

Morphological changes in neuronal cells were evaluated using a standard cresyl violet staining protocol.

Data analysis. A Two-way repeated ANOVA and a Mann-Whitney *U*-test were used for statistical analysis to evaluate the differences between the sham- and RF-exposed groups. A value of $p<0.05$ was considered statistically significant.

Results

Temperature conditions. Temperatures in the target area and rectum were measured during exposure to ensure that the findings of this experiment would not be distorted by thermal conditions caused by RF exposure at 2.0 W/kg TASAR (Figure 2).

At the beginning of exposure, basal temperatures in both regions were stabilized, without any significant difference between sham- and RF-treated groups (n=3 animals per group). The average temperatures in the target area in sham- and RF-treated groups were 34.9±0.5˚C and 35.1±0.2˚C, respectively. The average rectal temperatures for these groups were 36.5±0.4˚C and 36.7±0.3˚C, respectively.

During RF exposure at 2.0 W/kg TASAR, temperatures in the target area and rectum decreased slightly after 50 min of exposure in both groups. However, there was no significant difference in temperature between the two groups during the time-course of exposure (Figure 2A). The findings suggested that local RF exposure at 2.0 W/kg did not cause any elevation in temperature.

There was a clear relationship between TASAR of 10-min RF exposure and temperature changes in the target area and rectum, but only in the RF-treated group. The TASARs required to elevate temperatures were 20 W/kg or more for the target area and 200 W/kg or more for the rectum (Figure 2B).

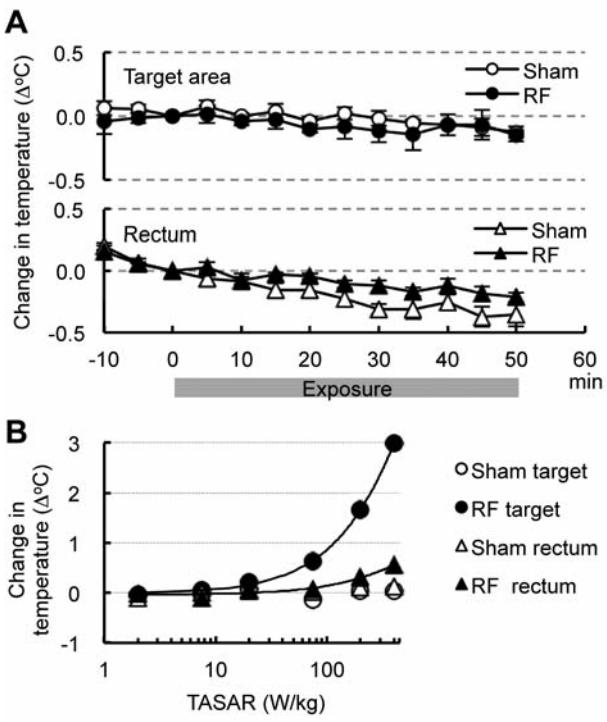

Figure 2. *Temperature changes in the target area and rectum under radiofrequency electromagnetic field (RF) exposure. The optical fiber thermometer probes were placed into the target area (cortex tissue) and the rectum. Temperatures in both regions were measured simultaneously before and during exposure. A: Change in temperatures during exposure at 2.0 W/kg of specific absorption rate in the target area (TASAR). There were no significant differences in either temperatures between sham- and RF-exposed groups (n=3 animals per group). B: Relationship between TASAR and temperature changes. The value shows the temperature changes during 10 min RF exposure at several TASARs. Values are mean (n=2 to 3 animals per group). Values are the mean±SEM.*

Changes in BBB permeability. To investigate whether BBB permeability was modified under local RF exposure at 2.0 W/kg TASAR, the fluorescence dye FITC-dextran (70 kDa) was injected intravenously before exposure and variations in fluorescence intensity in the target area were measured.

In a positive control using mannitol treatment, extravasation of the fluorescent dye was observed under an intravital microscope in real time (Figure 3A). The dye diffused into the parenchyma around the microvessels and accumulated in them. This accumulation of dye was detected as an increase in fluorescence intensity in the target area (Figure 3B).

In contrast, no extravasation of fluorescent dye was observed in any region of the target area in either group (Figure 3A, n=9 animals per group). Fluorescence intensity simply decreased time-dependently during the observation period, which was attributed to the dye clearing from the plasma (14). In addition, there was no significant difference in intensity of fluorescence between the two groups. These results showed that no change in BBB permeability to FITC-dextran was caused by local RF exposure at 2.0 W/kg TASAR.

Hemodynamic changes in pial venules. To determine whether cerebral hemodynamics related to BBB permeability were also modified under local RF exposure, we measured vessel diameter and blood flow velocity as hemodynamic parameters in pial venules during local RF exposure at 2.0 W/kg TASAR.

No significant dilation or constriction was observed in either post-capillary or collecting venules during RF exposure (Figure 4A). In addition, there was no significant difference in this parameter between sham- (108 venules in nine animals) and RF-treated (104 venules in nine animals) groups throughout the experiment. In sham- and RF-treated groups, 58 and 43 post-capillary venules were selected,

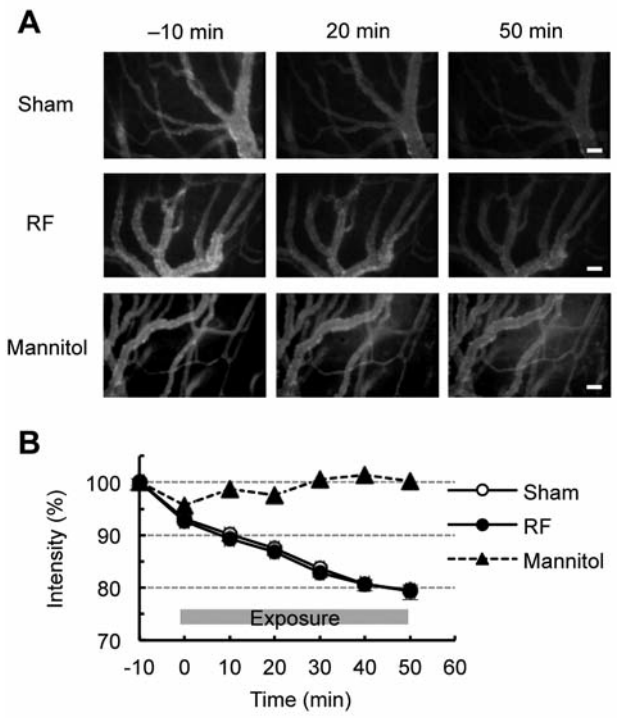

Figure 3. *Effect of radiofrequency electromagnetic field (RF) exposure on the blood–brain barrier. A: Representative fluorescence images of the target area. Fluorescent dye (fluorescein isothiocyanate-dextran, 70 kDa) was intravenously injected into the rats 25 min before RF exposure. Images were recorded every 10 min after dye injection under an intravital fluorescence microscope. No extravasation of the dye was observed in sham- nor RF-exposed rats, while dye leakage from microvessels to the parenchyma was detected in the osmotic shock model (n=1 animal) using mannitol treatment. Bar: 50 μm. B: Time-course of fluorescence intensity in the target area. Intensity was monitored and averaged in regions of interest (1–3 per animal) in the target area. No increase in average intensity was found in either sham- or RF-exposed rats, but did occur in the mannitol-treated animal, indicating an accumulation of extravasated dye. No significant differences were found between the sham- and RF-exposed groups (n=9 animals per group). Values are the mean±SEM, except for the mannitol-treated animal.*

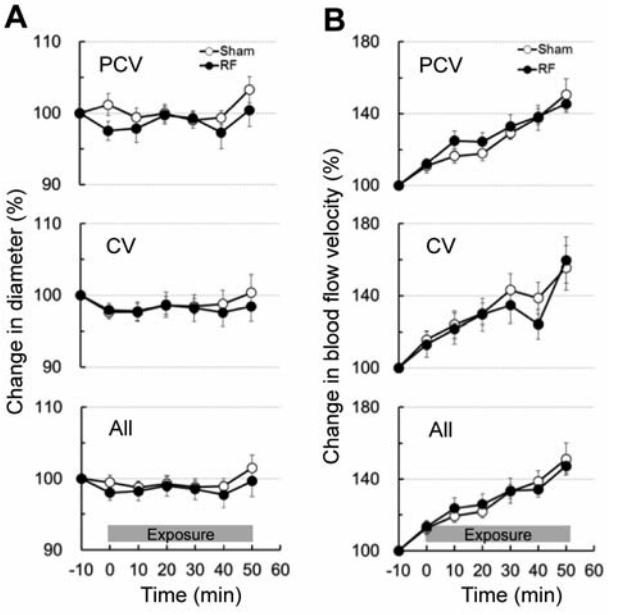

Figure 4. *Effects of radiofrequency electromagnetic field (RF) exposure on hemodynamic changes in pial venules. A: Change in diameter of pial venules. The diameter of post-capillary (PCV; 8≤d<30 μm) and collecting venules (CV; 30≤d≤50 μm) within the target area was measured. There were no significant differences in the diameters in PCV, CV, or overall (PCV + CV) between the sham- and RF-exposed groups (n=9 animals per group). B: Change in blood flow velocity in pial venules. The plasma velocity was measured in PCV and CV within the target area. No significant differences in plasma velocity were found in PCV, CV, or overall between the sham- and RF-exposed groups (n=8-10 animals per group). Values are the mean±SEM.*

respectively. In addition, 50 and 61 collecting venules were selected, respectively. There were no significant differences in diameter of each venule type between the two groups. These results did not reveal any change in venule diameter due to local RF exposure at 2.0 W/kg.

An increase in blood flow velocity was observed in post-capillary and collecting venules during RF exposure (Figure 4B). However, there was no significant difference in the velocity change between the sham-treated (96 venules in 10 animals) and RF-treated (87 venules in nine animals) groups throughout the experiment. In sham- and RF-treated groups, 69 and 60 post-capillary venules were selected, respectively. In addition, 27 collecting venules were selected in each group. There was no significant difference in the velocity change In each venule type between the two groups during exposure. These results revealed that no change in blood flow velocity was caused in the pial venules by local RF exposure at 2.0 W/kg.

Histological evaluation. If microcirculatory parameters, such as BBB permeability were modified during RF exposure at 2.0 W/kg TASAR, some traces caused by this modification would be found in the brain immediately after exposure. For this reason we examined stained brain sections using several histological methods.

Traces of changes in BBB permeability were immunohistochemically assessed by measuring the extravasation of serum albumin from cerebral vessels and number of neurons indicating albumin intake (Figure 5A). No immunostained sites or neurons were found in any of the brain sections of animals in either group (two regions in three animals per group), except in the circumventricular organs, which have no BBB function (Figure 5D). Therefore,

no statistical analysis was required to compare the serum leakage in the two groups.

Morphological differences in neuronal cells were also examined in brain sections stained with cresyl violet (Figure 5B). However, there were no changes in morphology related to RF exposure. Dark staining as a marker of shrunken neurons was only rarely present in RF-exposed brain sections and was not correlated with exposure.

Degenerated neurons were detected in the brain sections stained with Fluoro-Jade B (Figure 5C). No stained neurons were found in any of the brain sections in either group (two regions in three animals per group), while there were stained neurons in the section prepared as a positive control following hyperthermia (Figure 5E).

These results showed that no traces of cerebral inflammation remained, even after RF exposure at 2.0 W/kg.

Discussion

This *in vivo* study using real-time observation in rats produced three main findings. Firstly, the RF exposure, which was localized in a target cortex area at 2.0 W/kg TASAR, did not induce any temperature elevation in the target at any time during the experiment. Secondly, no extravasation of intravenously injected fluorescent dye was observed during exposure. Thirdly, no significant differences between sham- and RF-exposed rats were found either in blood flow velocity or in the diameter of the pial venules.

The figure-8 loop antenna used in these experiments provided effective local exposure of the rat parietal cortex. The exposure intensity in the target cortex area was estimated to be 90-fold that in the whole body in our dosimetry results (20). In previous local exposure systems targeting the whole brain (22-24), the ratio of brain- to whole-body-SAR ranged from 7 to 20. Thus, the disparity in intensity of our systems was 4 to 13-fold larger than that of the previous systems. This larger disparity in exposure intensity reflected very low rat whole-body exposure. Indeed, in our study, RF exposure at 200 W/kg TASAR or more was needed to detect any elevation in rectal temperature, whereas exposure at around 20 W/kg TASAR was sufficient to detect an elevation in the target area. Furthermore, our previous study, using a similar local exposure with 2.0 GHz RF, found that exposure even at 130 W/kg TASAR did not elevate the temperature of calf hypodermis (25). Therefore, it seems likely that the physiological responses in this study were obtained with little direct effect on whole-body exposure, including heat generation on the body surface.

As well as minimizing the direct effects of whole-body exposure, the aim was also to avoid increasing the temperature in the target area in order to focus on non-thermal physiological changes due to RF exposure. High-intensity RF exposure is known to generate heat in the brain,

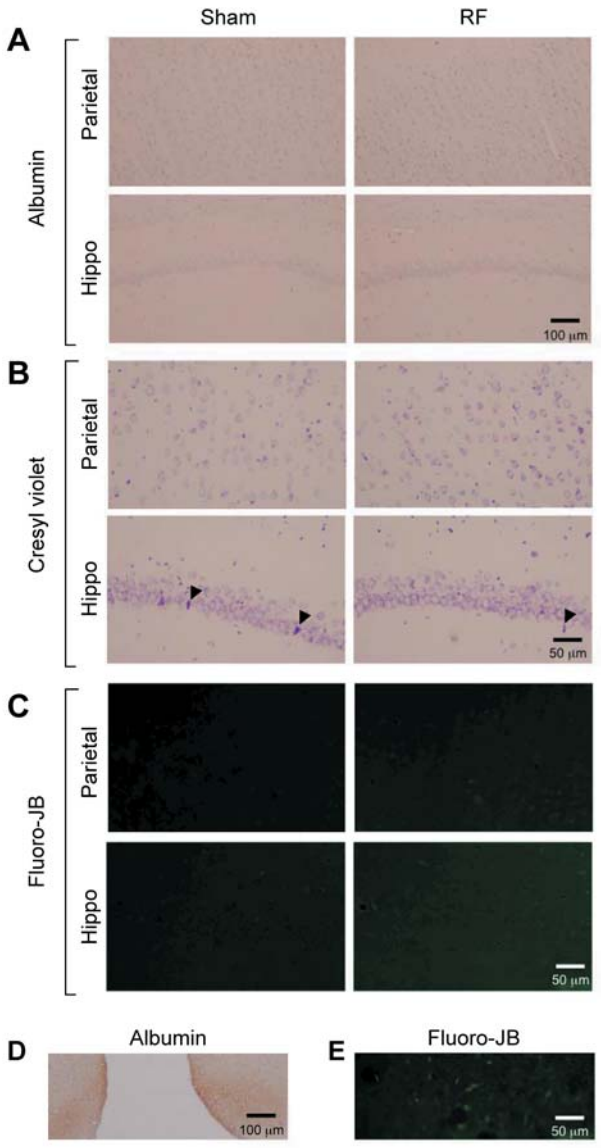

Figure 5. *Histological evaluation. Rat brains were fixed with 4% paraformaldehyde immediately after radiofrequency electromagnetic field (RF) exposure and sections were prepared for histological evaluation. Representative images (A-C) show the cortex of the target area and the hippocampus (hippo) below the target area. A: Immunohistological evaluation of serum albumin leakage sites. No immunostained sites with staining by albumin antibodies were observed in either sham- or RF-exposed groups. B: Cresyl violet-stained brain section. Dark neurons (arrow head) stained with cresyl violet were only rarely observed in the two groups. However, there were no morphological changes related to RF exposure. C: Fluoro-Jade B-stained brain section. Fluoro-Jade B-stained cells, indicating degenerated neurons, were not observed in either group. D and E are positive control images for serum albumin and Fluoro-Jade B, respectively. Immunostaining with antibody to albumin (brown color) was observed in a part of the pituitary region (circumventricular organs), which has no blood–brain barrier. Several cells were stained with Fluoro-Jade B (green color) in the cortex affected by hyperthermia.*

accompanied by several physiological changes, such as disruption of the BBB (26, 27) and an increase in blood flow (28). The TASAR value of 2.0 W/kg was chosen in order to eliminate such heat-induced effects. This SAR is the current restriction value (averaged over 10 g tissue for head and trunk) for local exposure to RF in the ICNIRP guidelines (1) and has been demonstrated not to elevate the temperature of human brain tissue (<0.2˚C) (29). Therefore, many human and animal experiments investigating the physiological effects of exposure have used the value of 2.0 W/kg SAR or less. However, few of them have measured the temperature in target tissues/organs during exposure, although temperature data are important for distinguishing thermal from non-thermal effects. This study certainly confirmed that RF exposure at 2.0 W/kg TASAR did not elevate temperatures, in either the target area or the rectum, throughout the experiment. Thus, all our findings were obtained under non-thermal conditions.

It has been argued whether BBB permeability increases and serum albumin extravasates into the brain parenchyma during RF exposure. Only few researchers have found evidence that low-intensity RF exposure induced serum albumin leakage in the rat brain (30-32). For example, Salford *et al*. found albumin leakage sites in rat brains following exposure to 915 MHz RF at less than 0.2 W/kg average whole-body SAR, suggesting that this exposure had disrupted the BBB (2). Unfortunately, their report did not indicate the average brain SAR. However, according to two confirmatory reports, the average brain SAR that Salford *et al*. used is estimated at 91-93% of average whole-body SAR (16, 18). Thus, it is suggested that this albumin leakage occurred under exposure at less than 0.19 W/kg average brain SAR. In contrast to their findings, many other investigators failed to confirm reproducible, conclusive effects, even following exposure at the local exposure limit (2 W/kg) (11, 16-18). Furthermore, Lin *et al*. suggested that only very high intensity exposure (>240 W/kg local peak SAR in rat brain) disrupted the BBB, due to hyperthermia (26). This local SAR is considerably above the local exposure limit. Nevertheless, some uncertainties have yet to be settled, particularly concerning possible transient changes in BBB that disappear immediately after exposure. Research has mainly focused on post-exposure effects, paying little attention to BBB permeability during RF exposure.

Our findings make a useful contribution to this issue, as no extravasation of FITC-dextran was confirmed in real time in the live rat cortex during RF exposure, even at 2.0 W/kg TASAR. This indicates that no extravasation of serum albumin was likely to have occurred, as FITC-dextran was selected (MW: 70000) for having approximately the same molecular weight as serum albumin (MW: 66000). Indeed, immunohistological examination revealed no traces of leakage of endogenous serum albumin in the target area nor in other exposed brain regions. Moreover, neither morphological changes nor degeneration of neuronal cells were found in the exposed brains, although extravasated serum albumin is known to lead to neurotoxicity in the brain parenchyma (5, 33). Of course, these histological parameters may be unsuitable for detecting transient effects on the BBB. However, no traces of albumin leakage or degenerated neurons seem to be circumstantial evidence of our findings obtained in real-time measurement. In our previous study using the same exposure system, no change in the permeability of the blood cerebrospinal fluid barrier for FITC-albumin was found in live rats during 30 min RF exposure at 0.5 W/kg brain-averaged SAR (TASAR: 1.9 W/kg) (34). Therefore, all these findings suggest that cerebral vessel permeability to serum albumin is not modified by RF below the local exposure limit (2 W/kg), even during local exposure.

It has been suggested that RF exposure modifies brain hemodynamics under non-thermal conditions. This phenomenon was identified in the human brain using positron-emission tomography, but is also somewhat controversial. Huber *et al*. initially found that rCBF increased after local RF exposure at 1.0 W/kg local SAR for 10 g brain tissue (4). On the contrary, Aalto *et al*. found an inverse effect: a local decrease in rCBF during RF exposure at 0.743 W/kg local SAR (35). However, two recent studies failed to confirm these effects. Mizuno *et al*. used exposure at 2.02 W/kg local SAR, about 2-fold higher than the other groups, and found no change in rCBF during nor after exposure (13). Ghosn *et al*. did not measure any changes in blood flow in the middle cerebral artery during or after exposure at 0.49 W/kg local SAR, using transcranial Doppler sonography (36). Cerebral blood flow is essential for neuronal activity and metabolism in the brain. Therefore, further research to confirm these phenomena is required, not only in humans but also in animals.

The data obtained in this animal study clarify this issue. The CCW method in rats facilitated direct monitoring of blood flow velocity and vessel diameter in the RF exposure target area. There was no difference in blood flow velocity between sham- and RF-treated groups during local exposure at 2.0 W/kg, although the velocity in both groups increased, which seemed to be related to changes in depth of anesthesia. Furthermore, no changes in diameter were observed in any pial venules during exposure. These two hemodynamic parameters are known to reflect rCBF. Of course, these data were obtained in rats, but certainly support the findings of Mizuno *et al*. concerning the absence of effects of RF.

In contrast, exposure to high-intensity RF has the capacity to increase CBF due to heating. For example, in our previous study using rats, local cortex exposure to 2.0 GHz RF at 10.5 W/kg TASAR for 18 min increased rCBF by 20% (25). However, in this case, the local increase in CBF was accompanied by a temperature elevation in the target cortex.

Using a microwave hyperthermia device, Moriyama *et al*. found a linear relationship between the increase in temperature and rCBF changes in monkey brains (28). These findings suggest that CBF changes during local RF exposure may be attributed to heat generation. This study focused on non-thermal effects of RF. Indeed, no temperature elevation was measured in target cortex tissue during exposure. Thus, exposure to low-intensity RF, not accompanied by any temperature elevation in tissues/organs, has no direct impact on hemodynamics. However, further local exposure investigations in the 2-10 W/kg range are required, as this seems to represent a boundary between non-thermal and thermal exposure conditions.

In conclusion, this research explored dynamic changes in cerebral microcirculatory parameters, BBB permeability, and hemodynamics in rat brains during local cortex exposure to RF under non-thermal conditions. However, no dynamic changes occurred in these parameters related to RF during 50 min exposure at 2.0 W/kg TASAR. Like many other research groups, we found that local RF exposure at these intensity levels had no impact on these parameters. Therefore, RF exposure below the local exposure limit (2 W/kg) is unlikely to induce dynamic or delayed effects on cerebral microcirculation. However, further investigation is required, under other experimental conditions, such as using juvenile animals.

Competing Interests

The Authors have declared that no competing interests exist.

Acknowledgements

This study was supported by the Ministry of Internal Affairs and Communications, Japan. We thank Mrs.' Miyuki Takahashi, Ritsuko Sasaki, Yoshiko Suzuki, Kasumi Yamanaka, and Minako Segawa for their helpful assistance.

Refferences

1 International Commission on Non-Ionizing Radiation Protection (ICNIRP): Guidelines for limiting exposure to time-varying electric, magnetic, and electromagnetic fields (up to 300 GHz). Health Phys *74*: 494-522, 1998.

2 Salford LG, Brun A, Sturesson K, Eberhardt JL and Persson BR: Permeability of the blood–brain barrier induced by 915 MHz electromagnetic radiation, continuous wave and modulated at 8, 16, 50, and 200 Hz. Microsc Res Tech *27*: 535-542, 1994.

3 Persson BR, Salford LG, Brun A, Eberhardt JL and Malmgren L: Increased permeability of the blood–brain barrier induced by magnetic and electromagnetic fields. Ann NY Acad Sci *649*: 356-358, 1992.

4 Huber R, Treyer V, Schuderer J, Berthold T, Buck A, Kuster N, Landolt HP and Achermann P: Exposure to pulse-modulated radio frequency electromagnetic fields affects regional cerebral blood flow. Eur J Neurosci *21*: 1000-1006, 2005.

5 Hassel BR, Iversen EG and Fonnum F: Neurotoxicity of albumin *in vivo*. Neurosci Lett *167*: 29-32, 1994.

6 Zlokovic, BV: Neurovascular pathways to neurodegeneration in Alzheimer's disease and other disorders. Nat Rev Neurosci *12*: 723-738, 2011.

7 Olesen J: Cerebral and extracranial circulatory disturbances in migraine: pathophysiological implications.Cerebrovasc Brain Metab Rev *3*: 1-28, 1991.

8 Charles A: The evolution of a migraine attack – a review of recent evidence. Headache *53*: 413-419, 2013.

9 Attwell D, Buchan AM, Charpak S, Lauritzen M, MacVicar BA and Newman EA: Glial and neuronal control of brain blood flow. Nature *468*: 232-243, 2010.

10 Zonta M, Angulo MC, Gobbo S, Rosengarten B, Hossmann KA, Pozzan T and Carmignoto G: Neuron-to-astrocyte signaling is central to the dynamic control of brain microcirculation. Nat Neurosci *6*: 43-50, 2003.

11 Tsurita G, Nagawa H, Ueno S, Watanabe S and Taki M: Biological and morphological effects on the brain after exposure of rats to a 1439 MHz TDMA field. Bioelectromagnetics *21*: 364-371, 2000.

12 Franke H, Ringelstein EB and Stogbauer F: Electromagnetic fields (GSM 1800) do not alter blood–brain barrier permeability to sucrose in models *in vitro* with high barrier tightness. Bioelectromagnetics *26*: 529-535.

13 Mizuno Y, Moriguchi Y, Hikage T, Terao Y, Ohnishi T, Nojima T and Ugawa Y: Effects of W-CDMA 1950 MHz EMF emitted by mobile phones on regional cerebral blood flow in humans. Bioelectromagnetics *30*: 536-544, 2009.

14 Masuda H, Ushiyama A, Hirota S, Wake K, Watanabe S, Yamanaka Y, Taki M and Ohkubo C: Effects of acute exposure to a 1439 MHz electromagnetic field on the microcirculatory parameters in rat brain. In Vivo *21*: 555-562, 2007.

15 Masuda H, Ushiyama A, Hirota S, Wake K, Watanabe S, Yamanaka Y, Taki M and Ohkubo C: Effects of subchronic exposure to a 1439 MHz electromagnetic field on the microcirculatory parameters in rat brain. In Vivo *21*: 563-570, 2007.

16 De Gannes FP, Billaudel B, Taxile M, Haro E, Ruffie G, Leveque P, Veyret B and Lagroye I: Effects of head-only exposure of rats to GSM-900 on blood-brain barrier permeability and neuronal degeneration. Radiat Res *172*: 359-367, 2009.

17 McQuade JM, Merritt JH, Miller SA, Scholin T, Cook MC, Salazar A, Rahimi OB, Murphy MR and Mason PA: Radiofrequency-radiation exposure does not induce detectable leakage of albumin across the blood–brain barrier. Radiat Res *171*: 615-621, 2009.

18 Masuda H, Ushiyama A, Takahashi M, Wang J, Fujiwara O, Hikage T, Nojima T, Fujita K, Kudo M and Ohkubo C: Effects of 915 MHz electromagnetic-field radiation in TEM cell on the blood–brain barrier and neurons in the rat brain. Radiat Res *172*: 66-73, 2009.

19 Masuda H, Ushiyama A, Hirota S, Lawlor GF and Ohkubo C. Long-term observation of pial microcirculatory parameters using an implanted cranial window method in the rat. In Vivo *21*: 471-479, 2007.

20 Arima T, Watanabe H, Wake K, Masuda H, Watanabe S, Taki M and Uno T: Local exposure system for rats head using a figure-8 loop antenna in 1500-MHz band. IEEE Trans Biomed Eng *58*: 2740-2747, 2011.

21 Hirota S, Masuda H, Ushiyama A, Asano M and Ohkubo C: Dual-slit photometric measurement of blood flow velocity by direct plasma fluorescence in rat pial maicrovessels. Microcirculation Annual. M. Asano and T Tamamoto (eds.). Nihon-Igakukan, Tokyo, Japanpp. 95-96, 2004.
22 Swicord M, Morrissey J, Zakharia D, Ballen M and Balzano Q: Dosimetry in mice exposed to 1.6 GHz microwaves in a carrousel irradiator. Bioelectromagnetics *20*: 42-47, 1999.
23 Chou CK, Chan KW, McDougall JA and Guy AW: Development of a rat head exposure system for simulating human exposure to RF fields from handheld wireless telephones. Bioelectromagnetics Suppl *4*: 75-92, 1999.
24 Leveque P, Dale C, Veyret B and Wiart J: Dosimetric analysis of a 900-MHz rat head exposure system. Microwave Theory and Techniques, IEEE Transactionson *52*: 2076-2083, 2004.
25 Masuda H, Hirata A, Kawai H, Wake K, Watanabe S, Arima T, Poulletier de Gannes F, Lagroye I and Veyret B: Local exposure of the rat cortex to radiofrequency electromagnetic fields increases local cerebral blood flow along with temperature. J Apply Physiol *110*: 142-148, 2011.
26 Lin JC and Lin MF: Microwave hyperthermia-induced blood–brain barrier alterations. Radiat Res *89*: 77-87, 1982.
27 Moriyama E, Salcman M and Broadwell RD: Blood–brain barrier alteration after microwave-induced hyperthermia is purely a thermal effect: I. Temperature and power measurements. Surg Neurol *35*: 177-182, 1991.
28 Moriyama E: Cerebral blood flow changes during localized hyperthermia. Neurol Med Chir *30*: 923-929, 1990.
29 Hirata A, Fujimoto M, Asano T, Wang J, Fujiwara O and Shiozawa T: Correlation between maximum temperature increase and peak SAR with different average schemes and masses. IEEE Trans Electromagnet Compat *48*: 569-578, 2006.
30 Salford LG, Brun AE, Eberhardt JL, Malmgren L and Persson BR: Nerve cell damage in mammalian brain after exposure to microwaves from GSM mobile phones. Environ Health Perspect *111*: 881-883, 2003.
31 Eberhardt JL, Persson BR, Brun AE, Salford LG and Malmgren LO: Blood-brain barrier permeability and nerve cell damage in rat brain 14 and 28 days after exposure to microwaves from GSM mobile phones. Electromagn Biol Med *27*: 215-229, 2008.
32 Nittby H, Brun A, Eberhardt J, Malmgren L, Persson BRR and Salford LG: Increased blood-brain barrier permeability in mammalian brain 7 days after exposure to the radiation from a GSM-900 mobile phone. Pathophysiology *16*: 103-112, 2009.
33 St'astny F, Skultetyova I, Pliss L and Jezova D: Quinolinic acid enhances permeability of rat brain microvessels to plasma albumin. Brain Res Bull *53*: 415-420, 2000.
34 Ushiyama A, Masuda H, Hirota S, Wake K, Kawai H, Watanabe S, Taki M and Ohkubo C: Biological effect on blood cerebrospinal fluid barrier due to radio frequency electromagnetic fields exposure of the rat brain *in vivo*. The Environmentalist *27*: 489-492, 2007.
35 Aalto S, Haarala C, Brück A, Sipilä H, Hämäläinen H and Rinne JO: Mobile phone affects cerebral blood flow in humans. J Cereb Blood Flow Metab *26*: 885-890, 2006.
36 Ghosn R, Thuroczy G, Loos N and Brenet-Dufour V: Effects of GSM 900 MHz on middle cerebral artery blood flow assessed by transcranial doppler sonography. Radiation Res *178*: 543-550, 2012.

Received November 10, 2014
Revised November 18, 2014
Accepted November 19, 2014